Structural Behavior of 45-Degree Underreamed Footings

SHAMIM A. SHEIKH AND MICHAEL W. O'NEILL

In this paper is described an experimental and analytical study aimed at developing a better understanding of the structural behavior of 45-degree underreamed footings. Two instrumented 45-degree footings 7.5 ft (2.29 m) in diameter with shafts 2.5 ft (0.76 m) in diameter were load tested under differing geotechnical conditions. One footing was situated in a very stiff clay, and the other was placed on a stratum of clay shale. In both tests failure occurred because of either bearing capacity failure of the footing itself or pullout failure of an anchor shaft. The footings sustained mean net bearing pressures of 100 psi (clay) and 157 psi (clay shale) without developing observable structural distress. Finite element analyses predicted well the measured base pressure distribution and the load-settlement characteristics of the footings; however, the maximum predicted tensile stresses in the underream under the imposed loads exceeded the tensile strength of concrete beam specimens tested to failure in flexure. Because no tensile cracking was actually observed in the test footings, a more realistic tensile strength criterion that relates to the status of stress in the footing needs to be established.

Ongoing research suggests that shallow foundations are as reliable as deep foundations for the support of bridge structures in many situations. One efficient way of constructing a shallow footing in cohesive soil is to machine-excavate an underream at a shallow depth and to concrete the excavation without reinforcing the bell. This raises the issue of footing capacity being controlled by structural strength rather than soil bearing capacity. Historically, to avoid premature structural failure, bridge engineers have either specified conical underreams with angles of 60 degrees (with the horizontal) or have disallowed unreinforced underreamed footings altogether. Unfortunately, the use of 60-degree underreams often requires more concrete than a spread footing constructed in the usual manner, and the diameter of the footing that can be excavated with mobile truck-mounted drilling equipment is quite limited. On the other hand, it is possible to construct 45-degree conical underreams to a diameter of 10 ft (3.05 m) or more with truck-mounted equipment and to reduce by one-third the volume of concrete required in the underream, which makes 45-degree underreamed footings economically viable alternatives to spread footings. To realize the benefits of using 45-degree underreams, factors that affect their structural capacity must be understood.

A recent study *(1)* has suggested that 45-degree underreamed footings may be considerably weaker structurally than 60-degree underreams. On the basis of a series of tests conducted in a laboratory environment on small-scale footings and associated analytical work, it was concluded that 45-degree underreams can fail at a uniform bearing pressure in the range of 8 to 12 ksf (0.34 to 0.43 MPa), whereas the bearing stress at failure in 60-degree underreams varied between 16 and 20 ksf (0.77 and 0.96 MPa). Failure initiated in most footings at the base because of tensile cracks in the concrete. Tand and O'Neill *(2)* conducted elastic finite element analyses of a 45-degree underreamed footing along with the surrounding soil, with similar results. The findings of these two studies have resulted in most designers specifying 60-degree bells for resisting high bearing stresses.

The purpose of this research was to experimentally and analytically study the behavior of 45-degree underreams in a field environment. The experimental part of the study involved the testing of two full-scale instrumented underreamed footings. Each footing had a 2.5-ft (0.76-m) nominal shaft diameter and a 7.5-ft (2.29-m) nominal bell diameter. One footing, tested in Houston, Texas, at the University of Houston-University Park Foundation Test Facility, was 7.75 ft (2.36 m) deep and founded on overconsolidated Beaumont clay, a Pleistocene soil deposited in a deltaic environment. The bearing stratum for the second footing, which was 12.5 ft (3.81 m) deep, was Eagle Ford shale, a Cretaceous clay-shale of marine origin. The site of this test was the grounds of Southwestern Laboratories, Inc., in Dallas, Texas.

In the analytical part of the study a finite element model of the 45-degree footing and the surrounding soil was developed. Stress-strain properties of Beaumont clay were used in the analysis to evaluate the behavior of the soil surrounding the footing. After a reasonable approximation of the behavior of the footing-soil system was established from the analytical work, the same discretization was used to analyze the two footings without the surrounding soil. A comparison of the experimental and the analytical results is presented in this paper for the tests conducted during this study as well as for tests reported earlier *(1)*.

GEOTECHNICAL CONDITIONS

The soil at the test site for Footing 1 (Houston) is in the Beaumont clay formation, which was heavily preconsolidated by desiccation. Extensive soil tests have been conducted at this site *(3)*. The undrained shear strength profiles for the depth of primary interest, as obtained from the UU triaxial compression tests and static cone penetration test (CPT) soundings *(4)*, are shown in Figure 1. The undrained shear strength profile for the

University of Houston-University Park, Houston, Tex. 77004.

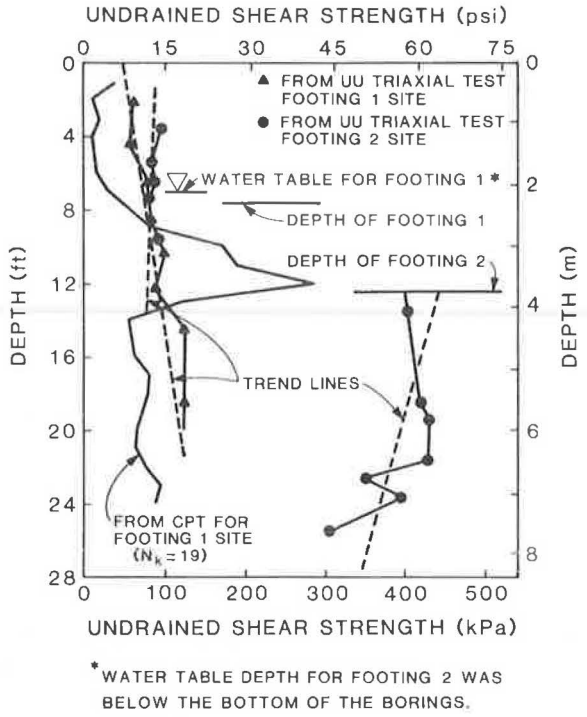

FIGURE 1 Undrained shear strength profiles.

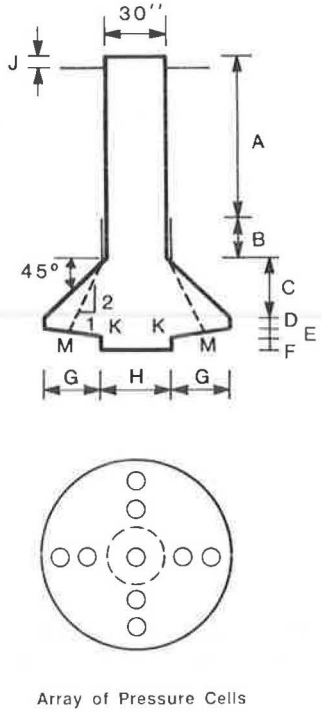

	FOOTING	
	1	2
A (in)	54.8	96.0
B * (in)	10.7	8.0
C (in)	29.9	35.0
D (in)	1.7	1.5
E (in)	0.0	2.0
F (in)	7.1	4.0
G (in)	32.3	29.5
H (in)	30.5	33.0
J (in)	4.1	- 1.5

1 in. = 25.4 mm

* Unbonded Concrete Outside Cardboard Tube.

FIGURE 2 Details of test footings.

CPT was obtained by dividing total cone tip pressures minus hydrostatic pore water pressures by a factor $N_k = 19$. The CPT profile suggests the presence of a soil layer of high undrained shear strength just below Footing 1. However, the high indicated shear strength values are manifestations of the presence of sand partings and calcareous nodules, which probably have little influence on the actual bearing capacity of the footing *(5)*.

On the same figure the variation with depth of the undrained shear strength of the soil at the Dallas site, as obtained from UU triaxial tests, is also shown. There is a sudden break in the strength profile at a depth of about 12.5 ft (3.81 m), below which hard blue clay shale exists. The soil above this depth was dark brown to gray clay fill. Both types of soil at this site, clay and shale, possess quite high degrees of preconsolidation. The unconfined compressive strength of the shale, the bearing stratum for Footing 2, is estimated at more than 100 psi (0.73 MPa) from the tests conducted on samples from the borings.

DETAILS OF TESTING

Details of the two test footings are shown in Figure 2. The depths of the footings were selected at the depth of the shallowest strong bearing stratum. The dimensions of the underreams, shown in Figure 2, were measured from within the excavations just before concreting. To break the bond between the concrete and the surrounding soil along the straight shaft portion of the footing, cardboard tubes with inside diameters of 2.5 ft (0.76 m) were used in both footings. In the case of Footing 1, there was no gap between the cardboard tube and the surrounding soil, which caused some side shear development at low values of applied load along the shaft. In the case of Footing 2, the borehole was 34 in. (0.86 m) in diameter, which resulted in an air gap of just under 2 in. (51 mm) between the outside of the tube and the surrounding soil.

Ready-mix concrete with a nominal compressive strength of 3,000 psi (20.7 MPa) at 28 days was used in both footings. Slight vibration was provided to assure concrete free of honeycombing. Footings 1 and 2 were tested 69 and 63 days after casting, respectively. The compressive strength of concrete samples was measured using standard 6- × 12-in. (152- × 305-mm) cylinders, and modulus of rupture was determined from 6- × 6- × 20-in. (152- × 152- × 508-mm) beams. At the time of testing, the actual compressive and tensile strengths of concrete used in Footing 1 were 3,970 and 538 psi (27.4 and 3.71 MPa), respectively. Using an 18 percent coefficient of variation between the laboratory and in situ concrete strengths *(6)*, the most probable lower limits of in situ compressive strength and modulus of rupture can be estimated at 3,255 and 441 psi (22.4 and 3.0 MPa), respectively. For Footing 2, the corresponding laboratory and lower limit of in situ compressive and tensile strength values for the concrete were 4,680 and 696 psi (32.3 and 4.8 MPa) and 3,840 and 570 psi (26.5 and 3.9 MPa), respectively.

The reinforcement cage in both of the footings consisted of eight No. 7 deformed steel bars, equally spaced around the circumference, and No. 3 ties at 6-in. (152-mm) spacing. Because it was observed during the testing of Footing 1 that some load transfer to the soil took place along the straight portion of the shaft, two opposite bars in Footing 2 were instrumented with eight strain gauges to evaluate the variation of load along the depth. The strain gauge data confirmed that no load transfer along the straight portion of Footing 2 took place.

In both footings, an array of nine total pressure cells 9 in. (229 mm) in diameter was used at the contact between the base of the footing and the soil, as shown in Figure 2. All nine cells

in Footing 1 and four cells in Footing 2 were of the pneumatic type. The other five cells in Footing 2 were of the vibrating-wire type. All pneumatic cells were calibrated up to a pressure of 140 psi (0.96 MPa), and the vibrating-wire cells were calibrated up to a pressure of 150 psi (1.0 MPa). All of the cells used exhibited linear behavior, which allowed extrapolation of the data with some confidence during the footing test for one of the vibrating-wire cells that recorded a pressure of about 180 psi (1.24 MPa).

To measure the movement of the base, two telltales were used in each footing. Movements of the base and the top of each footing were measured using four dial indicators with least counts of 0.001 in. (0.025 mm). The reference frames used for these measurements were anchored to the ground at a distance of about 10 ft (3.05 m) on each side of the center of the footings.

Two underreamed drilled shaft anchors with shafts 2.5 ft (0.76 m) in diameter, bells 7.5 ft (2.29 m) in diameter, and depths of 18 ft (5.49 m) were used for the application of load on Footing 1. These anchor shafts were installed at a distance of 9.5 ft (2.9 m) from the center of the test footing. The anchor shafts for Footing 2, situated 9 ft (2.75 m) from the center of the test footing, were cylindrical shafts 4 ft (1.22 m) in diameter and 30 ft (9.14 m) deep. The movements of the anchor shafts were monitored continuously during both tests. The test setup for Footing 1, showing the reaction beams, is shown in Figure 3.

FIGURE 3 Overall test setup for Footing 1.

Footing 1 was loaded to 500 kips (2224 kN) in 100-kip (445-kN) increments, beyond which the loading increment was reduced to 50 kips (222 kN). After each 100-kip (445-kN) increment, load was maintained for 60 min; after each 50-kip (222-kN) increment, the load was maintained for 30 min. The loading steps for Footing 2 were 100, 300, 500, 650, 750, 850, 950, and 1,040 kips (445, 1335, 2224, 2892, 3336, 3780, 4226, and 4626 kN). Each load level except the last was maintained for 60 min. Most of the readings were taken at 2, 29, and 59 (if any) min after the application of a load increment.

RESULTS

It was stated earlier that the use of the cardboard tube in the shaft portion of Footing 1 may not have completely broken the bond between the concrete and the soil. It is also plausible that load was transferred from the roof of the underream to the overlying soil through suction. Figure 4 compares two curves, top load versus base settlement and base load versus base settlement, for Footing 1 that indicate that initially very little of the applied load reached the bearing surface. The difference between the top load and the base load (load transferred above the base) is also shown in the same figure. The maximum non-base-bearing load transfer occurred at a settlement of about 0.5 percent of the base diameter, beyond which the shaft bond or roof suction, or both, broke, and essentially all of the load was thereafter transferred to the bearing surface.

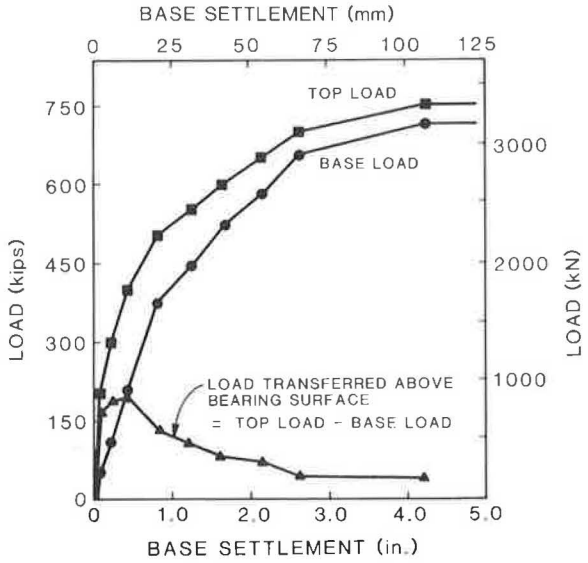

FIGURE 4 Transfer of load in Footing 1.

The base load in Figure 4 was calculated as the summation of the product of average base pressures and the areas over which each average pressure acts. Details are available elsewhere *(4, 7)*. The variations of the contact pressure along the radius of the base, based on the average of the readings taken during the time a particular load was maintained, are shown in Figure 5 for various top-load levels for both footings. The base pressures are reasonably uniform for both footings, although the soil characteristics at the two bases were significantly different. A tendency of higher stresses close to the circumferences of the bases is consistent with the elastic continuum solution. Three-dimensional plots of the distribution of net base pressures for the two footings at their maximum loads are shown in Figure 6. The distribution appears reasonably uniform except for the east-west direction in Footing 2. This was probably because on the east side there was about 6 to 12 in. (152 to 305 mm) of fill material between the base of the footing and the shale. This soft material resulted in lower stiffness on the east side and hence lower bearing stresses. The average stress in the east-west direction is, however, almost equal to that in the north-south direction.

In both footings, no sudden variations were observed in the base pressure readings during testing, which indicated that no

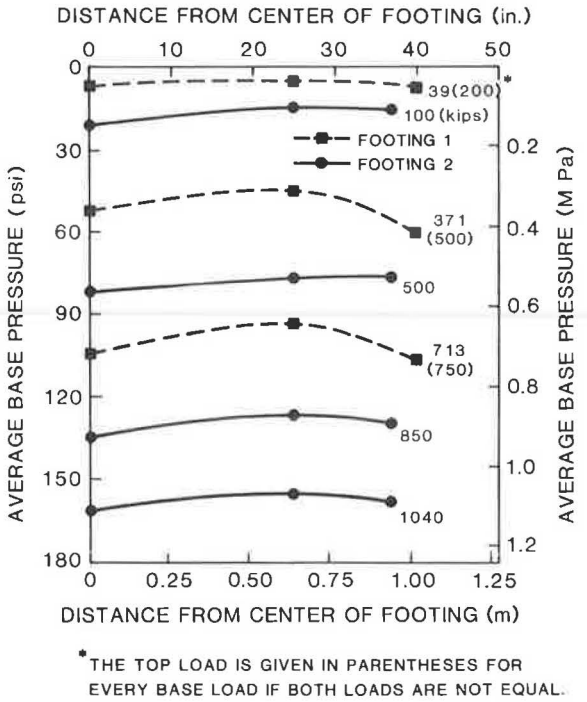

FIGURE 5 Average net base pressure for various loads.

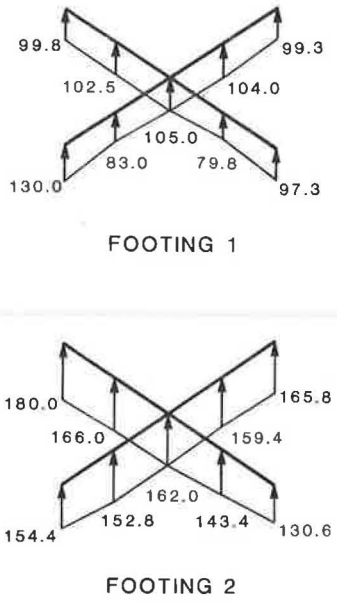

FIGURE 6 Variation of base stress (psi) at maximum loads.

sudden changes of stiffness of the footings took place during the course of loading, and hence no tensile cracking of concrete occurred in the bell.

The base load versus base settlement curves for the two footings are shown in Figure 7, in which significantly higher initial stiffness of the bearing surface for Footing 2 with respect to Footing 1 and a lack of any appreciable stiffness reduction up to the maximum pressure experienced are quite obvious.

Although one of the main purposes of this work was to evaluate the structural capacity of 45-degree underreams and to study the failure mechanism in the bell, both tests had to be terminated because of failure in the soil. The structural capacity of Footing 1 exceeded the estimated value based on the available information on 45-degree underreams *(1, 2)*. The most convenient location for the test was the University of Houston Foundation Test Facility, where the net ultimate bearing capacity of the near-surface soil is about 15 ksf (0.72 MPa). This soil capacity was twice the average stress at which Farr reported that most model footings failed structurally *(1)*. In addition, at

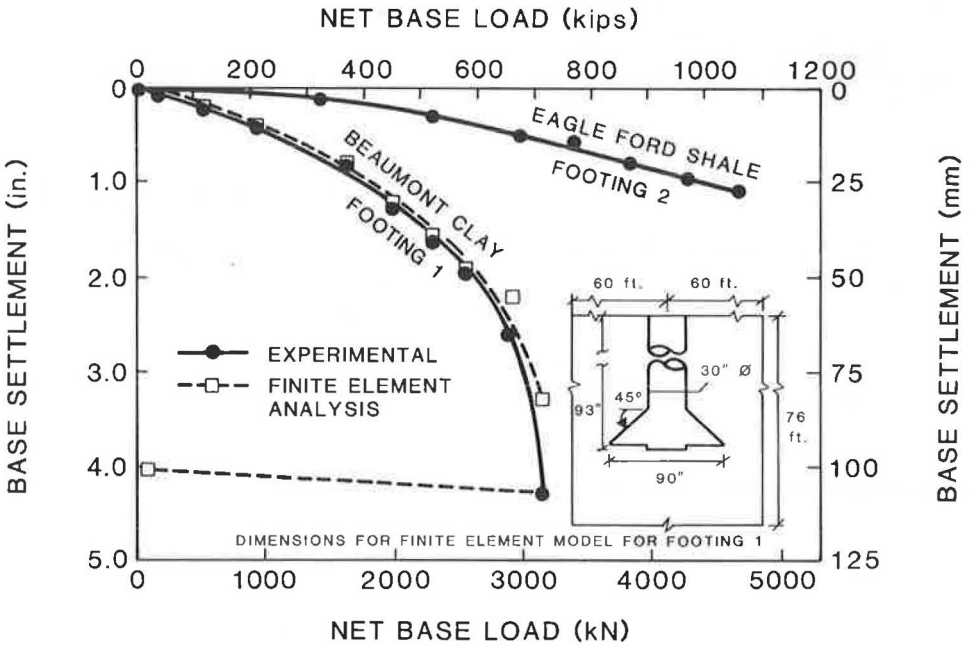

FIGURE 7 Comparison of experimental and analytical net base load versus base settlement.

this bearing stress the maximum analytically determined tensile stress in bell concrete exceeds the largest of the tensile strengths measured from available laboratory tests.

The second test was planned for a maximum load of 2,000 kips (8900 kN) to produce a bearing stress of about 300 psi (2.1 MPa). The anchor shafts were designed on the basis of the commonly used undrained adhesion of 28 psi (193 kPa) for the blue shale in the Dallas area. The shearing resistance offered by the top 10 ft (3.1 m) of clay fill as well as the suction developed at the base of the reaction shafts were neglected to provide an apparently conservative design. One of the anchor shafts, however, failed at a total load of about one-half the maximum design load. At a footing load of 950 kips (4226 kN), the anchor shaft started failing, and between 950 and 1,040 kips (4226 and 4626 kN) the uplift movement increased from 0.126 in. (3.2 mm) to 0.524 in. (13.3 mm). The test was terminated because the load could not be maintained beyond this point. At failure, the average side shear in the lower 20 ft (6.1 m) of the shaft was only about 14 psi (97 kPa). The load-uplift behavior of the two anchor shafts for Footing 2 is shown in Figure 8.

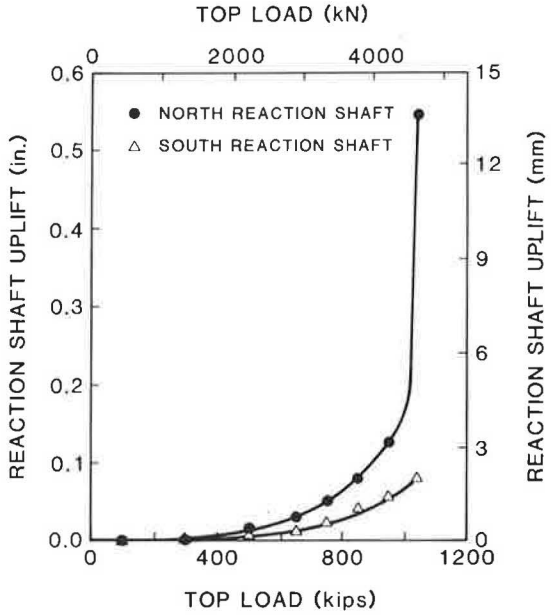

FIGURE 8 Uplift of reaction shafts versus top load on Footing 2.

COMMENTARY ON TEST RESULTS

Structural failure of an underreamed footing is most likely to initiate at the base. Simple analyses for flexural or diagonal tension failure, following the logic applied to the analysis of single column footings, ideally can be carried out to estimate the onset of failure. Flexural failure may cause the initiation of cracking at the point of maximum moment (Point K in Figure 2). Based on the maximum measured base pressure, the upper limits on the flexural stresses in Footings 1 and 2 are 399 and 460 psi (2.75 and 3.17 MPa), respectively. The lower limit on the modulus of rupture of concrete is estimated at 441 and 570 psi (3.04 and 3.93 MPa) for Footings 1 and 2, respectively. Flexural failure was therefore not imminent.

Diagonal tensile stresses are assumed to initiate cracks at the base at Point M (Figure 2). The maximum values of these stresses for Footings 1 and 2 were calculated to be 135 and 169 psi (0.93 and 1.17 MPa), respectively. These stresses are considerably less than the shear strength of concrete in these footings, which is estimated at least to be equal to $4\sqrt{f_c'}$ (f_c' in psi) or at least 228 psi (1.58 MPa) in Footing 1.

Standard simplified analysis therefore would not appear to predict structural failure in the two footings tested at the values of the loads applied.

FINITE ELEMENT ANALYSIS

A finite element study of the footing-soil system was carried out to supplement the experimental results. A commercially available ANSYS software package was used for analysis. By taking advantage of the axial symmetry of the structure and the loading, only one radial wedge of the structure and soil was discretized, and two-dimensional axisymmetric elements were used for both soil and concrete over the entire region of interest. Because the main purpose of the study was to investigate the underream, the soil-structure interaction along the straight side of the shaft was not included in the analysis. Gap elements were introduced along the interface between soil and concrete and also placed horizontally in the soil region close to the level of the shaft base. This was done to release the erroneously high tensile stresses in the soil and to simulate approximately the development of soil cracks in the tension zones. The gap elements were released in shear initially along the shaft and at the roof of the underream. Gap elements at the base of the underream were released when the interface shear stress exceeded the undrained shear strength of the soil.

The complete finite element mesh is shown in Figure 9. Figure 10 shows the detailed discretization of the bell region. The size of the elements used is reduced in the area of high stress concentration. To reflect the actual observed field measurements, the notch (Point K in Figure 2) was chamfered as shown in Figure 10. The centerline of the shaft was constrained against horizontal movement, and the bottom and side boundaries were completely fixed.

Mechanical properties of both soil and concrete were estimated from the results of the laboratory sample tests. Nonlinear material characteristics were modeled as bilinear stress-strain curves. Properties were assumed to be identical in both tension and compression. For concrete, the initial stiffness of 390,000 ksf (18 670 MPa) was used up to a von Mises yield stress of 400 ksf (19.2 MPa), beyond which the stiffness was reduced to 78,000 ksf (3735 MPa). For the soil for Footing 1, the stiffness values used were 840 ksf (40 MPa) up to a von Mises yield stress of 4 ksf (0.19 MPa) and 42 ksf (2 MPa) beyond that. These properties were based on the standard concrete cylinder tests in compression and UU triaxial tests on soil specimens recovered from beneath the elevation of the bearing surface.

A comparison of the analytical and experimental base load–base settlement curves is shown in Figure 7 for Footing 1. An iterative procedure for analysis was employed to account for the inelastic material properties. In the initial stages of loading, the solution converged rapidly. At higher loads, however, the convergence required several iterations, particularly to satisfy

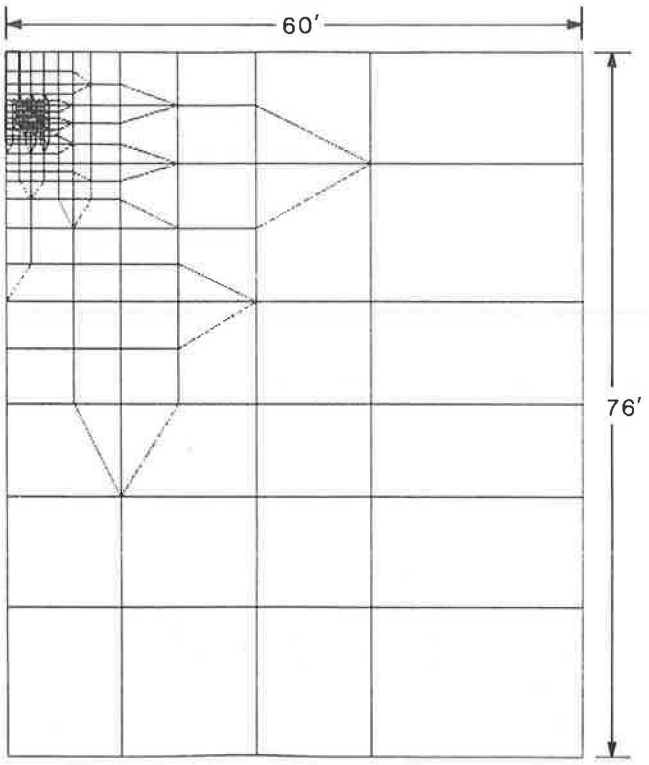

FIGURE 9 Full mesh for the shaft-soil system for Footing 1.

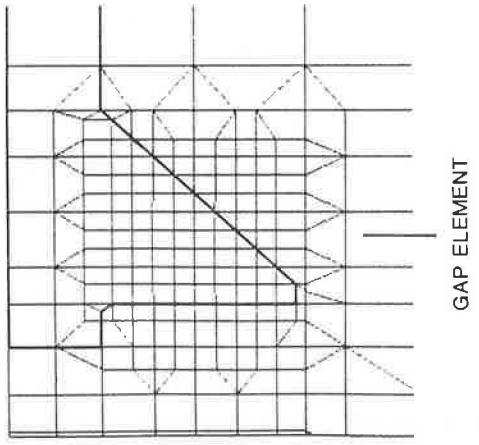

FIGURE 10 Enlarged portion of the mesh for the shaft-soil system for Footing 1.

limits on soil properties. Because of computer system limitations, it was therefore decided to relax the convergence criterion for the last two points on the analytical curve in Figure 7.

Analytical base reaction pressure distribution near the maximum load is compared with both the equivalent uniform pressure distribution and the measured values for Footing 1 in Figure 11. Analytical results compare well with measured values. However, at the notch, which is an area of stress concentration, the analytical solution indicates pressure almost twice the value of the uniformly distributed pressure. It should be noted that the base reaction was not measured directly at the

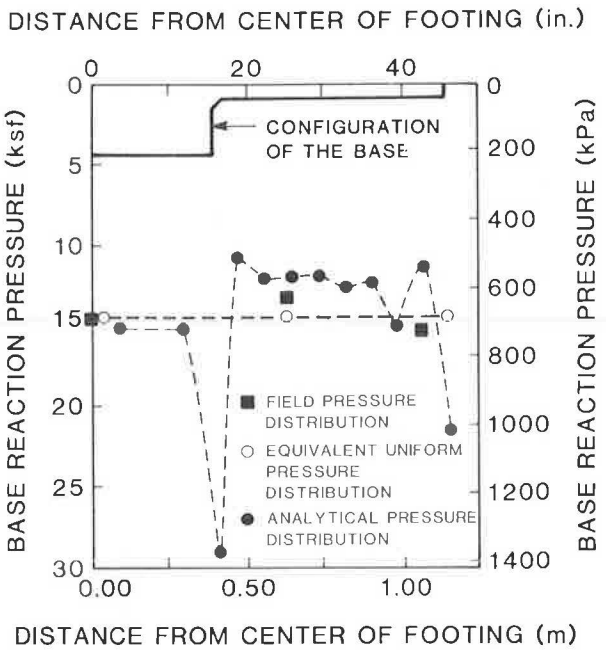

FIGURE 11 Base pressure distribution at base load of 713 kips in Footing 1.

notch. The analytical value may be more representative of the actual pressure in the notch area compared with either the average pressure or the pressure interpolated from the measured values.

Footings 1 and 2 were then analyzed without the surrounding soil, subjected to top load, and constrained by a uniform base pressure and no other surface tractions. The mesh of the concrete structure was not changed from the previous analysis because that mesh provided base pressure distribution and load-settlement behavior for Footing 1 that were reasonably close to the experimental results. Table 1 gives a comparison of the analytical and the experimental maximum stress values in concrete for footings tested during this study and the earlier laboratory study *(1)*.

When the soil was included in the mesh, the maximum calculated concrete tensile stresses in Footing 1 (just above the notch) were about 13 percent higher than those calculated without the soil. This difference can be explained by the higher Poisson's ratio of the nearly incompressible soil (0.45) compared with that of concrete (0.20). Maintenance of compatibility between soil and concrete at the base results in additional tensile stresses in the concrete. The maximum tensile stress under the maximum load in Footing 2, when analyzed with the surrounding soil mass, would therefore have been about 970 psi (6.69 MPa).

It is apparent that, for both of the footings tested during this investigation, the analysis predicted the occurrence of tensile stresses in the bell at the maximum base load that significantly exceeded the maximum tensile strength (modulus of rupture) of the concrete. Even then there was no cracking or other signs of distress in these footings, as was confirmed by careful observation of the footings after they were extracted and cleaned at the completion of the tests (Figure 12). For the reduced-scale tests reported earlier *(1)*, the calculated tensile stresses caused by

TABLE 1 MAXIMUM CALCULATED CONCRETE STRESSES

Full-Scale Tests	Base Load (kips)	Tensile[a] Stress (psi)	Tensile[a] Strength (psi)	Compressive Stress (psi)	Compressive Strength (psi)	Toe Height (in.)
Present investigation						
Footing 1[b]	713	668	565	1,323	3,960	7
	713	584	565	1,337	3,960	7
Footing 2	1,043	848	696	1,950	4,680	7
Model tests from Farr *(1)*						
Average of 7 tests	50.6[c]	371	315		4,234	0
Average of 5 tests	59.5[c]	534	395		4,974	3

[a]Tensile strength for Footings 1 and 2 refers to modulus of rupture. For other tests split tensile strength of concrete was reported, which is about 20 percent lower than modulus of rupture.
[b]Finite element analysis of the footing was performed with the surrounding soil in place. In all other cases soil was not included.
[c]At failure.

failure loads were found to be higher than the split cylinder strength of concrete and approximately equal to the modulus of rupture. The maximum compressive stresses in both of the footings in this study were found to be well below the concrete compressive strength.

The apparent difference between the results of the present investigation and those of the model tests of the earlier study *(1)* can be explained as follows.

The model footings were tested in a laboratory on a nonyielding bearing surface. This may have caused a concentration of bearing stresses that produced tensile stresses in excess of those calculated from the finite element analysis. The model footings were cast upside down, which may have resulted in weak concrete at the base due to bleeding and segregation. The unique features of the curing of the concrete in a saturated-soil environment and the confinement of concrete by the surrounding soil may have caused an improvement in the in situ properties of the concrete in Footings 1 and 2.

Tensile strength of concrete is commonly measured by application of direct tension, splitting a concrete cylinder by applying load along its length, or by the modulus of rupture test. Split cylinder strength and modulus of rupture strength are about 25 and 50 percent, respectively, higher than direct tensile strength. Recently Chen and Yuan *(8)* suggested a new indirect method for determining the tensile strength of concrete. In this method, known as the double punch method, a compressive load is applied to a concrete cylinder along its axis through two steel punches placed on the top and bottom surfaces of the cylinder. This results in an almost uniform tensile stress across all diametrical planes. The tensile strength of concrete was observed to be between $4\sqrt{f_c'}$ and $7\sqrt{f_c'}$ (f_c' in psi), which is comparable with the usual split cylinder strength of concrete.

Given such a large variation in the indicated tensile strength of concrete, which depends on several factors including the type of test (which determines the state of stress), size and shape of specimen, and shrinkage, it is difficult to estimate the in situ tensile strength of concrete in the footings.

In the analysis, although bilinear stress-strain curves were used for the material properties, stresses in concrete were still within the elastic range at maximum loads. Because of softening of concrete in both tension and compression, the stresses may be overestimated, although an attempt was made to reduce this overestimation by using a lower-limit value of initial stiffness of the concrete. [A ratio between the stresses calculated from an elastic analysis and actual stresses of 1.2 has been suggested for dams (*9*, p. 26).] It has also been suggested that the tensile stresses thus calculated should be compared with the split cylinder strength or the apparent stresses should be checked against the modulus of rupture *(10)*.

It appears that the tensile stresses in the footing concrete would be slightly lower than those calculated from finite element analyses. Even then, the stresses appear to have exceeded the modulus of rupture values for samples taken of the concrete in the footing. Because full-sized footings did not develop tensile failure, it appears that the in situ tensile strength is greater than that indicated by moduli of rupture of the samples. This conclusion suggests that a more realistic tensile strength criterion, which can account for the state of stresses in underreamed footings, needs to be established.

CONCLUSIONS

A well-formed 45-degree underreamed footing was capable of resisting base bearing pressure in excess of 157 psi (1.08 MPa) without structural failure or any other sign of structural distress.

In Beaumont clay the service limit load for the footings would be dictated by soil constraints and not by underream structural constraints. The finite element method, which accounts for the nonlinear behavior of soil, predicts the load-settlement behavior and the distribution of base bearing stresses in a reasonable manner.

The structural failure of the bell is more likely to be caused by the combined effects of flexure and shear than by flexure or punching shear alone.

The tensile stresses calculated under the maximum applied loads exceeded the maximum tensile strength of concrete as measured from flexure tests on samples from both of the footings. This indicates that the in situ tensile strength of the concrete in the underream is significantly higher than the sample modulus of rupture. A more realistic tensile strength criterion, which can account for the complex state of stress in the footings, is needed.

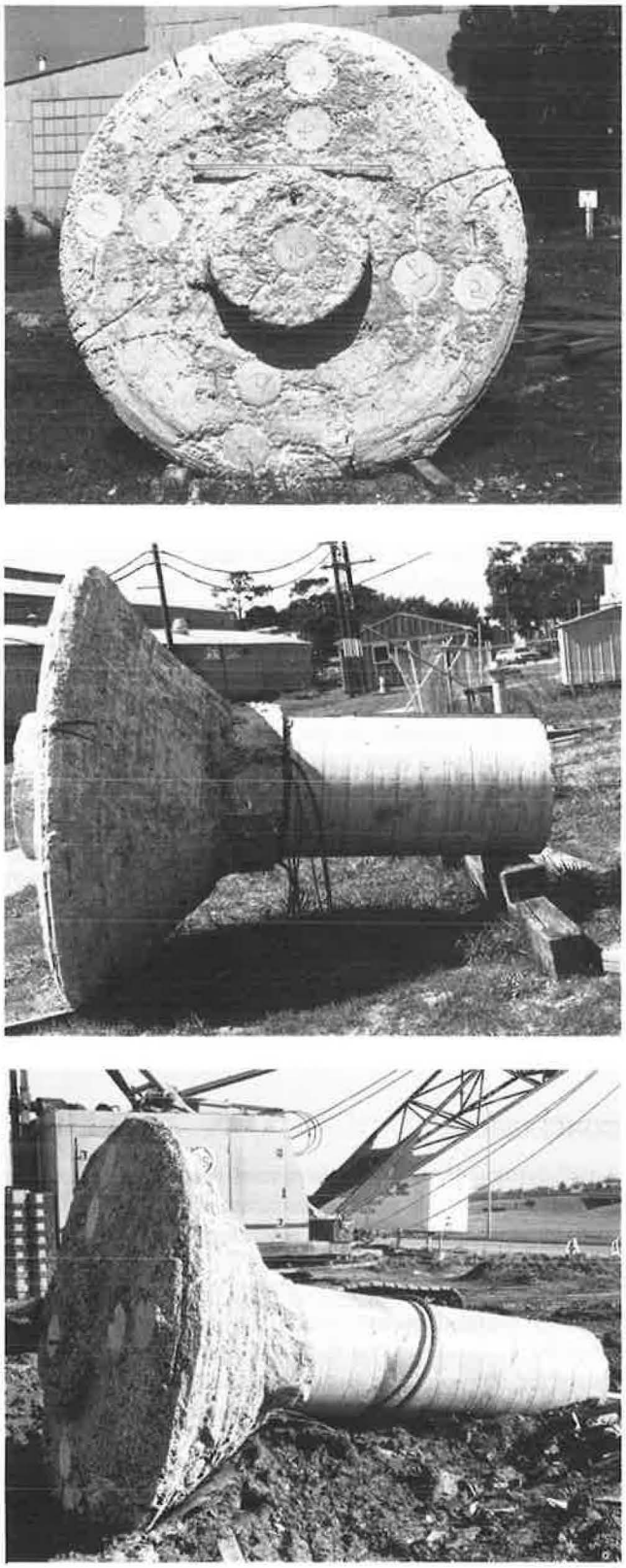

FIGURE 12 Extracted footings.

Further full-scale field tests, particularly tests conducted to structural failure, are needed to increase the confidence level in this type of foundation. However, it would appear, pending the development of new methods of evaluation of concrete tensile strength in underreams, that shallow 45-degree underreamed footings with concrete of the quality described here can be safely employed as bridge foundations at ultimate limit–state bearing pressures of the order imposed in the tests reported.

ACKNOWLEDGMENTS

The research reported here was supported in part by a grant from the International Association of Drilled Shaft contractors. The authors are grateful to Farmer Foundation Company of Houston and N. L. Schutte, Inc., of Dallas for providing drilling and concreting services and to Southwestern Laboratories, Inc., of Dallas for their technical support. The assistance of former graduate students Ketan Kapasi, David Menzies, N. Venkatesan, and Albert Wu in conducting the tests and analyses is also appreciated.

REFERENCES

1. J. S. Farr. Study of the Load Capacity of Plain Concrete Underreams. M.S. thesis. The University of Texas at Austin, 1974, 106 pp.
2. K. E. Tand and M. W. O'Neill. Prediction of Load-Settlement Response for Deep Footing. Preprint, ASCE, Tri-Sectional Meeting, Albuquerque, N.M., Oct. 1977, 22 pp.
3. L. J. Mahar and M. W. O'Neill. Geotechnical Characterization of Desiccated Clay. *Journal of Geotechnical Engineering,* ASCE, Vol. 109, Jan. 1983, pp. 56–71.
4. S. A. Sheikh, M. W. O'Neill, and N. Venkatesan. *Behavior of 45° Underreamed Footings.* Research Report UHCE 83-18. Department of Civil Engineering, University of Houston-University Park, Tex., Nov. 1983, 126 pp.
5. M. W. O'Neill and S. A. Sheikh. Geotechnical Behavior of Underreams in Pleistocene Clay. In *Drilled Piers and Caissons II* (C. B. Baker, Jr., ed.), ASCE, May 1985, pp. 57–75.
6. J. G. MacGregor, S. A. Mirza, and B. Ellingwood. Statistical Analysis of Resistance of Reinforced and Prestressed Concrete Members. *ACI Journal,* Vol. 80, No. 3, June 1983, pp. 167–176.
7. S. A. Sheikh, M. W. O'Neill, and K. J. Kapasi. *Behavior of 45° Underreamed Footing in Eagle Ford Shale.* Research Report UHCE 85-12. Department of Civil Engineering, University of Houston-University Park, Tex., Dec. 1985, 129 pp.
8. W. F. Chen and R. L. Yuan. Tensile Strength of Concrete: Double-Punch Test. *Journal of the Structural Division,* ASCE, Vol. 106, No. ST8, Aug. 1980, pp. 1673–1693.
9. *Feasibility Design Summary, Auburn Dam, Concrete Curved-Gravity Dam Alternative (CG-3).* Water and Power Resources Service, U.S. Bureau of Reclamations, Denver, Colo., Aug. 1980.
10. J. M. Raphael. Tensile Strength of Concrete. *ACI Journal,* Vol. 81, No. 2, March–April 1984, pp. 158–165.

Publication of this paper sponsored by Committee on Foundations of Bridges and Other Structures.